Reinforcing Additives for Ice Adhesion Reduction Coatings

Christopher J Wohl[1], Lilly L. Balderson[2], Devon M. Beck[2], Francisco A. Mendez Sosa[2], Yi Lin[3], and Joseph G. Smith Jr[1]
[1]NASA Langley Research Center, Hampton, VA, 23681, USA
[2]NASA Internship, Fellowship, and Scholarship Program, NASA Langley Research Center, Hampton, VA, 23681, USA
[3]National Institute of Aerospace, Hampton, VA, 23666, USA
c.j.wohl@nasa.gov

Introduction

Adhesion of contaminants has been identified as a ubiquitous issue for aeronautic exterior surfaces.[1-4] In-flight icing is particularly hazardous for all aircraft and can be experienced throughout the year under the appropriate environmental conditions. On larger vehicles, the accretion of ice could result in loss of lift, engine failure, and potentially loss of vehicle and life were it not for active de-icing or anti-icing equipment. Smaller vehicles though cannot support the mass and mechanical complexity of active ice mitigating systems and thus must rely upon passive approaches or avoid icing conditions altogether. One approach that may be applicable to all aircraft is the use of coatings.[5-7] Durability remains an issue and has prevented realization of coatings for leading edge contamination mitigation. In this work, epoxy coatings were generated as a passive approach for ice adhesion mitigation and methods to improve durability were evaluated.

Highly cross-linked epoxy systems can be extremely rigid, which could have deleterious consequences regarding application as a leading edge coating. Incorporation of flexible species, such as poly(ethylene glycol) may improve coating toughness.[8] Additionally, core-shell rubber (CSR) particles have been utilized to improve fracture toughness of epoxies.[9] Both of these more established additives are investigated in this work. An emerging additive that is also evaluated here is holey graphene. This nanomaterial possesses many of the advantageous properties of graphene (excellent mechanical properties, thermal and electrical conductivity, large surface area, etc.) while also exhibiting behaviors associated with flexible, porous materials (i.e., compressibility, increased permeation, etc.). Holey graphene, HG, was synthesized by the oxidation of defect-rich sites on graphene sheets through controlled thermal exposure.[10] It is envisioned that the porous nature of HG would allow resin penetration through the graphitic plane, resulting in better interfacial interaction and therefore better translation of the nanomaterial's properties to the surrounding matrix.

Experimental

Epoxy coatings were generated on prepared aluminum (Al) substrates of Al 3003 for Taber abrasion, Al 2024 for impact testing, and Al 6061 for ice adhesion testing. Surfaces were prepared by abrasion using a solution of Pace® B-82 (Chemetall®) diluted in water by a factor of 7 until a water break-free surface was observed. A solution of AC-131 (3M™), which had been mixed and agitated for at least 30 min, was applied to the surface.

Modified epoxy resins were prepared from the base resin (BR) combination of the diglycidyl ether of bisphenol A (DGEBPA, DER™ 331, Dow® Chemical) and 1,3-bis(4-aminophenoxy)benzene hardener at a hardener/epoxy (h/e) ratio of 0.8. Typically, 10 g of each formulation was prepared by adding each component into a plastic sample bottle and heating the mixture in an oil bath at 90°C for approximately 15 min with stirring following by cooling to room temperature for approximately 10 min. The resultant solution was coated onto prepared substrates by dispersion from a plastic syringe.

A glycidyl ether-terminated poly(ethylene glycol) (PEG, Aldrich, number average molecular weight ~ 500 g/mol) was incorporated at values ranging from 0-50 wt% while maintaining the same h/e ratio. These coatings are designated as BR-PEG$_{\#}$, where # indicates the PEG loading level. CSR particles dispersed in a DGEBPA resin (Kaneka Kane Ace MX-125) were also incorporated and the amount of DER™ 331 was adjusted to maintain the same h/e ratio. Designations of formulations with CSR particles (ranging from 0-10 wt%) are indicated with CSR$_{\#}$, where # indicates particle loading level. HG, dispersed in a minimal amount of N,N'-dimethylformamide (10 mg/mL; ~ 15 mL total) and sonicated for at least 1 h, was included in formulations at loading levels ranging from 0-1 wt%. No changes in reactive species quantities were made as HG was considered to be an inert additive. Formulations including HG are indicated with HG$_{\#}$, where # indicates the HG loading level.

PEG, CSR, and HG were added to the BR prior to heating. Coated substrates were held in a forced air chamber overnight to remove any volatile species and subjected to the recommended cure cycle for DER 331 (2 h at 100 °C followed by 4 h at 177 °C).

Advancing and receding water contact angles (θ_A and θ_R, respectively) were determined on a First Ten Angstroms FTA1000B according to ASTM D7334. A minimum of 3 water droplets were utilized for each surface and interfacial tension measurements were conducted prior to testing to verify the purity of the solvent and image resolution. Taber abrasion testing was conducted according to ASTM D4060

using a Qualitest GT-7012-T and H-18 Taber wheels. Tests were conducted using a custom sample support that enabled generation of approximately 3.73 cm diameter samples centered on the abrasion wheel wear path. Up to 1200 cycles were performed on each surface at 60 rpm. Coating thickness-dependent wear index (WI_T) was calculated according to equation 1, where W_0 and W_{1200} are the sample initial weight and weight after 1200 abrasion cycles, C is the number of cycles, and T is the coating thickness (thickness values ranged from 250 to 1500 μm as determined using a Checkline 3000FX coating thickness guage). Impact testing was performed according to ASTM D2794 using an Elcometer 1615 impact tester with a 1 kg drop weight and a 15.9 mm radius impact surface. Testing was conducted from a drop height of 40 cm on both coated and uncoated surfaces.

$$WI_T = \frac{(W_0 - W_{1200})1000}{C * T} \quad (1)$$

Ice adhesion strength (IAS) was determined on a custom-built laboratory scale ice adhesion testing device (AERTS Jr.) as has been described previously.[11] Impact ice was accreted at -16 °C with a calculated liquid water content (LWC) between 0.4-0.5 g/m^3 and droplet mean volumetric diameter of 20 μm. These conditions fall within the FAR Part 25/29 Appendix C icing envelope.[12] Both the epoxy-coated sample disk and a control disc (highly roughened such that ice would detach from the test surface first) were weighed and mounted onto an Al rotor that was subsequently mounted in the refrigerated centrifuge in AERTS Jr. The rotor was spun up to 5500 rpm (93 m/s) and thermally equilibrated at -16 °C for at least 20 min. Supercooled microdroplets were introduced through a NASA MOD 2 nozzle located above the plane of rotation. Ice release from the sample was detected by an accelerometer attached to a ballistic wall surrounding the centrifuge. The difference in accreted ice mass was equated to the shed ice mass from the sample surface which was utilized to calculate IAS according to equation 2 where m_{ice}, v, and r are the mass of shed ice, linear velocity at the sample surface, and the rotor radius, respectively.

$$IAS = \frac{m_{ice}v^2}{r} \quad (2)$$

Results and Discussion

Consideration of a coating formulation for application to a wing leading edge must involve a series of material properties including the intended functionality (contaminant adhesion prevention) as well as other service life requirements such as durability, mechanical properties, etc. The BR considered in this work was identified as exhibiting initial promise for reducing IAS (internal results). However, initial testing of this formulation for other required properties indicated that further formulation modifications would be necessary to realize this coating for application as a leading edge material. Figure 1 indicates the result of impact testing of an Al alloy coupon coated with the BR formulation. As seen, severe coating integrity failure was observed. However, inclusion of PEG dramatically improved the outcome of impact testing.

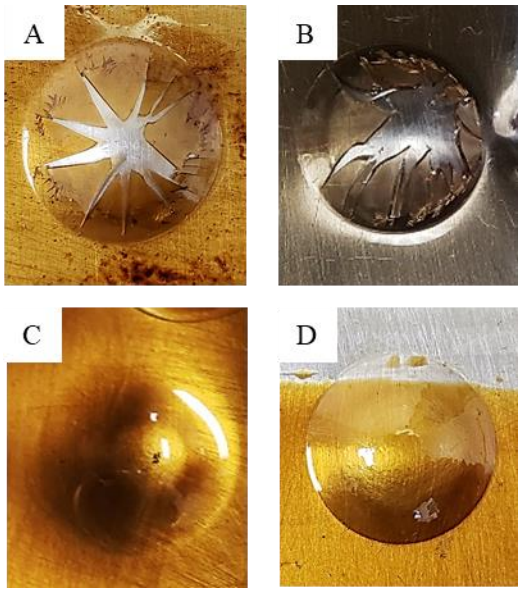

Figure 1. Impact testing of (A) BR, (B) BR-PEG$_{15}$, (C) BR-PEG$_{35}$, and (D) BR-PEG$_{50}$ according to ASTM D2794. The deformation width was approximately 16 mm.

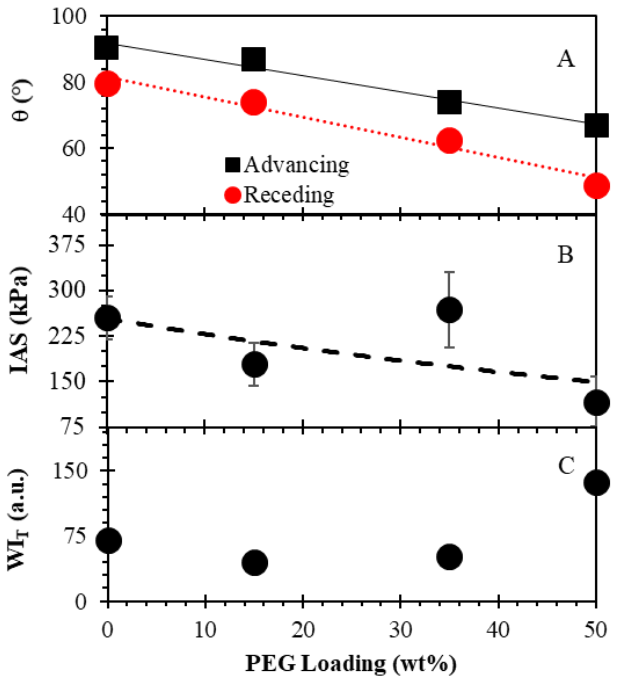

Figure 2. (A) Advancing and receding water contact angle values measured on PEG-containing epoxy coatings. (B) IAS values measured at -16 °C on PEG-containing epoxy coatings. (C) Thickness-dependent wear index values determined on PEG-containing epoxy coatings.

Based on the results of Figure 1, a series of modified BR formulations was prepared with varying amounts of PEG. These coatings were characterized with the results summarized in Figure 2. As could be anticipated, increasing PEG content resulted in a decrease in water contact angle

values due to PEG's hydrophilic nature (Figure 2A). Interestingly, increasing the PEG content resulted in a decrease in ice adhesion strength (Figure 2B). This can be related to molecular flexibility imparted by the PEG as well as known properties of PEG to act as a freezing point depressant for ice formation.[13] The exponential decay fit-line through the IAS data (Figure 2B) suggested that increasing PEG content should decrease IAS. Further, Taber abrasion results indicated that an increase in PEG content (50 wt%) resulted in a decrease in wear performance (Figure 2C). This can be related to the aliphatic nature of the PEG additive compared to the aromatic nature of the BR. Based on these results, the amount of PEG that should be included to improve impact test performance (fracture toughness) without adversely impacting wear performance was determined to be approximately 35 wt%. This formulation was utilized for the studies involving CSR and HG additives.

To ascertain the influence the additives had on coating performance, each additive was evaluated individually. A series of CSR-containing formulations was prepared and characterized according to the same procedures as those utilized on the PEG-containing formulations described previously. As can be seen in Figure 3, the CSR inclusion did not improve wear performance compared to the BR-PEG_{35} formulation, although IAS did improve in several cases. Conversely, inclusion of HG (at loading levels ≤ 0.25 wt%) resulted in both an improvement in IAS and wear performance at low loading levels. The gray box in Figure 3 is the region where formulations that exhibited an improvement in both properties, relative to BR-PEG35, would be located. At HG loading levels > 0.25 wt%, surface roughness increased (data not shown) and consequential embrittlement led to a reduction in wear performance. Impact testing performed on several formulations found that inclusion of CSR resulted in retention of the fracture toughness of the BR-PEG35 formulation (Figures 1C and 4A). Conversely, inclusion of HG, even at loadings as low as 0.1 wt%, resulted in a reduction in fracture toughness (Figures 1C and 4B).

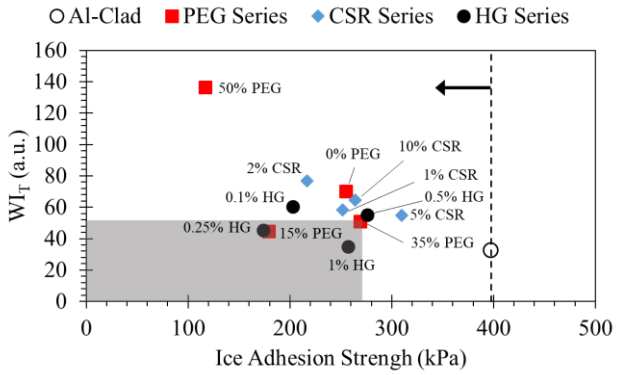

Figure 3. Comparison of IAS at -16°C and wear index for epoxy formulations containing varying amounts of PEG, CSR, and HG additives. The open circle is the value measured for an Alclad Al 2024 T3 surface. Coatings with improved performance, relative to the BR-PEG_{35} coating, would be located within the shaded regions.

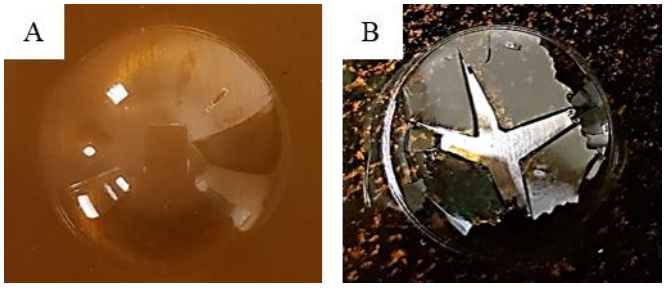

Figure 4. Impact testing of (A) BR-PEG_{35}-CSR_{10} and (B) BR-PEG_{35}-$HG_{0.5}$ conducting according to ASTM D2794. The deformation width was approximately 16 mm.

Summary

Through a series of tests involving IAS, Taber abrasion, and impact testing it was observed that there was an additive loading dependency. Improvement in one property was often at the expense of another using the BR-PEG_{35} resin. Inclusion of HG improved the wear performance and IAS but reduced the fracture toughness. Incorporation of CSR retained fracture toughness but diminished wear performance and IAS slightly. Combinations of these additives will be explored to determine if the best attributes of each can be incorporated into a promising formulation.

References

1. J.E. Seebergh, et al., Durable Exterior Coatings for the Next generation of Aerospace Finishing Systems. In *19th International Conference on Surface Treatments in the Aeronautics and Aerospace Industries (SURFAIR)*, Biarritz, France, 2012.
2. N. Dalili, et al., *Renewable Sustainable Energy Rev.* **2009,** 13, pp 428-438.
3. G. Fiore and M.S. Selig In *A Simulation of Operational Damage for Wind Turbine Blades*, 32nd AIAA Applied Aerodynamics Conference, Atlanta, GA, June 16-20; Atlanta, GA, 2014.
4. C. Laforte, et al., Icephobic Coating Evaluation for Aerospace Applications. In *AIAA SciTech Forum*, National Harobr, MD, 2014.
5. K.G. Krishnan, et al., *Appl. Surf. Sci.* **2017,** 392, pp 723-731.
6. C.J. Wohl, et al., Epoxy Composite Coatings to Mitigate Contamination of Aircraft Wing Leading Edges. In *39th Annual Meeting of the Adhesion Society*, San Antonio, TX, 2016.
7. K. Golovin, et al., *Science Advances* **2016,** 2, pp 1-12.
8. A.B. Cherian and E.T. Thachil, *Macromolecular Engineering* **2007,** 36, pp 128-133.
9. R. Bagheri, et al., *Polymer Reviews* **2009,** 49, pp 201-225.
10. Y. Lin, et al., *Advanced Functional Materials* **2015,** 25, pp 2920-2927.
11. J.G. Smith Jr, et al., Design and Development of a Laboratory-scale Ice Adhesion Testing Device. In *41st Annual Meeting of The Adhesion Society*, San Diego, CA, 2018.
12. R.K. Jeck, Icing Design Envelopes (14 CFR Parts 25 and 29, Appendix C) Converted to a Distance-Based Format. Federal Aviation Administration, 2002, COT/FAA/AR-00/30.
13. S.-C. Wang, et al., *Macromolecules* **2002,** 35, pp 9551-9555.